Versatile low-temperature atomic force microscope with *in situ* piezomotor controls, charge-coupled device vision, and tip-gated transport measurement capability

Jhinhwan Lee,[a] Jungseok Chae, Chung Koo Kim, Hyunjin Kim,[b] Seungeun Oh,[c] and Young Kuk[d]
Department of Physics, Seoul National University, Seoul 151-747, Korea

(Received 21 April 2005; accepted 11 July 2005; published online 23 August 2005)

A versatile cryogenic (5 K) ultrahigh-vacuum (UHV) atomic force microscope (AFM) with tip-gated transport measurement capability has been developed. Using high-resolution (<1.5 μm) plan-view charge-coupled device (CCD) optics, and three planar piezomotors we achieved visually guided *in situ* alignments of a sample position with respect to the AFM tip, and the laser beam position with respect to the cantilever and the quadrant photodiode. We made optical fiber feedthroughs and a laser lens assembly to bring external laser light and CCD illuminating light onto the cantilever and the sample. A sample holder with an embedded temperature sensor and eight transport electrodes is detachably mounted on a piezotube scanner. The generic cantilever mount can be easily replaced with a tuning-fork mount or a piezoresistive cantilever mount for experiments where stray laser light should be avoided. To our knowledge, this is the first Dewar-immersion type cryogenic AFM with laser beam deflection sensing capability and high-resolution plan-view CCD optics. © *2005 American Institute of Physics.* [DOI: 10.1063/1.2018352]

I. INTRODUCTION

Since the advent of atomic force microscope (AFM),[1] its ease of use and versatility has made it one of the most important and widely used tools in nanotechnology[2–4] and biotechnology.[5–7] Recently we have observed the increased need for AFM with a transport measurement capability operable in ultrahigh vacuum (UHV) at cryogenic temperatures and/or in high magnetic field environments for the investigation of various novel materials in various device geometries.[3,4,8–14] In this paper we report the construction of an AFM which can be operated in UHV at a cryogenic temperature of 5 K without sacrificing the ease of use of a room-temperature AFM and features simultaneous transport measurement for nanoelectronics research [such as scanning gate microscopy in two–dimensional electron gas (2DEG) or nanowires]. The AFM has adopted the Dewar-immersion configuration for optimal thermal stability and for possible use in a high-magnetic field Dewar. High-resolution plan-view charge-coupled device (CCD) optics and three planar piezomotors contribute to easy and fast *in situ* controls of the sample position and the laser beam alignment.

II. INSTRUMENT DESIGN

The AFM head has a rigid three-column construction, and is immersed in a liquid-helium Dewar and cooled by the helium exchange gas (at about 1/3 of atmospheric pressure) for optimal thermal and vibrational stability, as shown in Fig. 1. Five metallic baffles attached externally on the upper part of the main probe chamber reduce the convection of the helium exchange gas and reflect the radiation from the top flange of the Dewar. Radiation through the main probe chamber is effectively cut off by internal baffles and the objective lens of the CCD optics just above the head (to be described later). Attached on the top of the main probe chamber are an ion pump, a turbomolecular pump, an ion gauge, a CCD camera, and electrical/fiber feedthroughs. The whole UHV chamber sits on an air table on top of a heavy steel frame.

Most of the parts in the AFM head in Fig. 2 are made of vacuum-casted duralumin, an aluminum-copper alloy, for rigidity, machinability, and high thermal conductivity. We designed the head so that we can use many different types of cantilevers, such as standard laser-deflection-type cantilevers (contact and noncontact modes), piezoresistive cantilevers, and quartz tuning forks, by changing the endpiece of the cantilever holder and switching the electronics for the detection of the tip-sample interaction accordingly. In this paper we will mainly focus on the laser-deflection sensing type since it requires additional planar piezomotors for the laser and photodiode sensor. The head has four inertial piezomotors: one "Pan-type" one-dimensional (1D) Z motor[15] (10 mm span) for the sample coarse approach, and three planar

[a]Present address: Department of Physics, Cornell University, Ithaca, NY 14853.
[b]Present address: Department of Physics, Brown University, Providence, RI 02912.
[c]Present address: Department of Physics, Massachusetts Institute of Technology, Cambridge, MA 02139.
[d]Author to whom correspondence should be addressed; electronic mail: ykuk@phya.snu.ac.kr

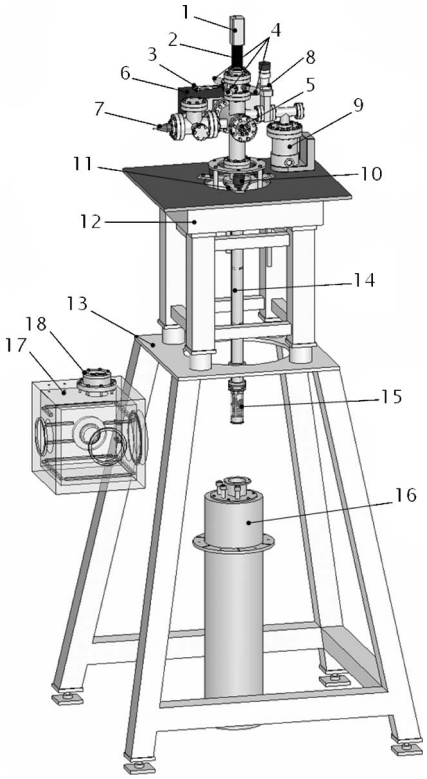

FIG. 1. Structure of the low-temperature AFM (LTAFM) system. (1) CCD camera, (2) telescopic zoom lens, (3) optical fiber feedthroughs, (4) electrical multipin feedthroughs, (5) BNC feedthroughs, (6) ion pump, (7) ion gauge, (8) gate valve, (9) turbomolecular pump, (10) air springs for Dewar, (11) bellows-type Dewar coupling, (12) air table, (13) main supporting frame, (14) main probe chamber, (15) LTAFM head, (16) liquid-helium Dewar, (17) glove box, (18) docking port for LTAFM head.

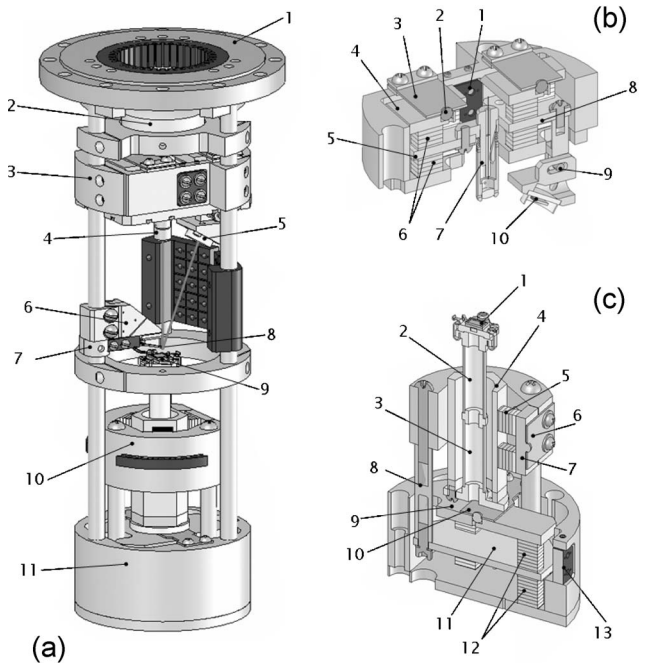

FIG. 2. (a) LTAFM Head. (1) 4 K plate, (2) objective lens for CCD optics, (3) 2D piezomotors for laser and quadrant photodiode, (4) laser lens assembly, (5) quadrant photodiode, (6) cantilever holder assembly, (7) cantilever holder stop, (8) cantilever, (9) sample, (10) *Z* sample walker (11) *XY* sample walker. (b) Laser and quadrant photodiode piezomotor assembly. (1) Connector block, (2) ruby ball, (3) BeCu spring, (4) top plate, (5) sapphire plate for laser, (6) shear piezo stacks, (7) fiber-laser lens assembly, (8) sapphire plate for quadrant photodiode, (9) position-angle adjustment screw, (10) quadrant photodiode. (c) Sample *XYZ* motor stage. (1) Sample holder assembly, (2) fine-*Z* piezotube, (3) *XY* and coarse-*Z* piezotube, (4) sapphire prism, (5) shear piezo stack, (6) BeCu spring, (7) side press plate, (8) *Z* walker support, (9) *XY* walker top plate, (10) BeCu spring, (11) sapphire plate for *XY* walker, (12) shear-piezo stacks for *XY* walker, (13) connector block.

XY motors (2 mm$\times$2 mm span each) for fine horizontal positioning of the sample and adjusting the laser lens assembly and the quadrant photodiode.

Each of the three planar piezomotors has six feet (three in the top plate pressed by a BeCu spring and three in the fixed bottom plate) that clamp and translate the moving polished sapphire plate, giving sufficient stability against vibration. Every foot of the motor is composed of either four (for laser and photodetector piezomotors) or eight (for the sample piezomotor) stacked shear piezos (EBL#3, Staveley Sensors) with dimensions 6 mm$\times$6 mm$\times$1 mm. The difference in the walking speeds in the *x* and *y* directions is less than 15%, and the angular deviation of the walking directions from the nominal *x* and *y* directions are less than 5°. A Pan-type linear walker with six independent shear piezo feet is used for coarse movement of the sample to the tip. Since the white light source (the cleaved end of the multimode fiber) illuminates the sample surface at an angle θ with $\tan\theta \sim 0.1$, we can estimate the distance between the tip and the sample to be ten times the distance between the cantilever and its shadow laid on the sample, achieving a safe and fast coarse approach down to $\sim$5 μm of the tip-sample distance.

The cantilever holder also has a rigid lightweight construction for maximum resonance frequency. A small U-shaped BeCu spring clamps the cantilever body with maximum force into a shallow mating groove made in the holder, so that the cantilever can be vibrated at high frequency (up to 500 kHz at 10 nm amplitude). The cantilever holder can be rotated about one half turn around a vertical column to a convenient cantilever exchange position. After the exchange of the cantilevers, the holder can be placed back in its original position with high repeatability guided by the vertical-and-rotational stop. The BeCu spring can be opened easily by inserting a surgical blade and gently twisting it. Its clamping force did not weaken after replacing more than 100 cantilevers. In the case of a piezoresistive cantilever holder, the BeCu spring holds the plate on which the cantilever is glued and wire-bonded and one can manually snap the cantilever plate in and out.

The sample holder has an embedded miniature temperature sensor (DT-470-SD, Lakeshore) just beneath a thin copper plate on which the sample die is glued (using E415G or T905-BN, Epoxy Technology, or an adhesive carbon tape, depending on detailed application), as shown in Fig. 3. The copper plate is thermally anchored to the surrounding duralumin ring by a fine wire copper braid. The sample holder is easily removed using a retaining ring remover and has eight gold-plated-copper electrodes that can be connected to electrodes on the sample die by wire-bonding. For air- or humidity-sensitive samples we can do most of the sample exchange procedures in a glove box that has a vertical docking port capable of mating with the AFM head.

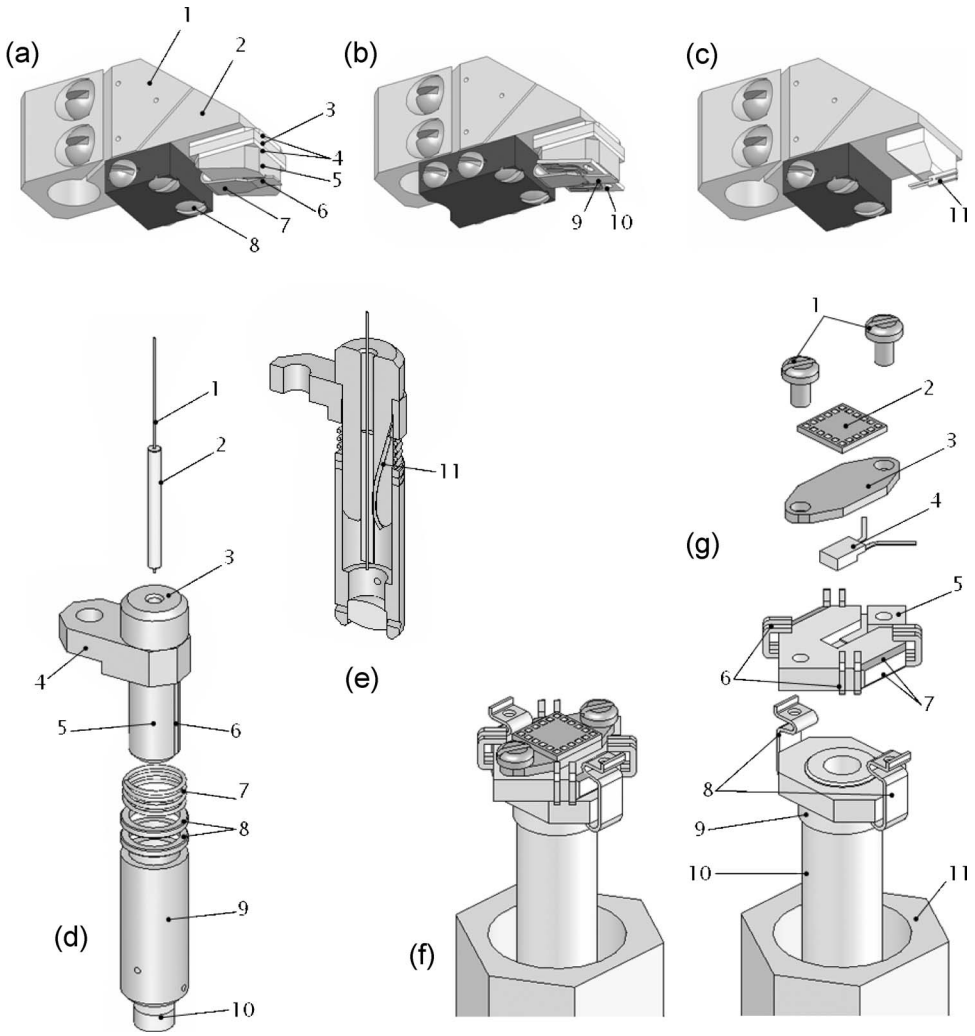

FIG. 3. Various cantilever holders for (a) standard contact/noncontact mode cantilevers, (b) nonstandard, actuated, or embedded-sensor (piezoresistive) type cantilevers, and (c) tuning-fork sensors. (1) Cantilever holder support, (2) removable cantilever holder, (3) piezo oscillator, (4) alumina plates, (5) cantilever mount, (6) cantilever, (7) BeCu spring, (8) connector block, (9) cantilever glued and wire-bonded to cantilever plate, (10) cantilever plate, (11) tuning fork. (d), (e) Laser lens assembly. (1) Single-mode optical fiber, (2) glass capillary, (3) fiber holder, (4) fiber holder support, (5) fine threads, (6) slot for fiber-holding Inconel spring, (7) helical Inconel spring, (8) washers, (9) lens tube, (10) focus lens, (11) fiber-holding Inconel spring. (f), (g) Sample holder. (1) Copper plate mount screw, (2) sample, (3) copper plate, (4) silicon diode temperature sensor, (5) macor sample holder body, (6) transport electrodes, (7) titanium metallized surfaces, (8) BeCu springs, (9) macor sample holder base, (10) piezotube scanner, (11) sapphire prism.

The laser light for cantilever deflection sensing and the white light for CCD illumination originate from a stabilized optical-fiber laser source ($\sim$630 nm, 0$\sim$2.5 mW variable intensity, S1FC635, Thorlabs) and a halogen light source external to the chamber through homemade optical fiber feedthroughs as shown in Figs. 2 and 3. The fiber feedthroughs were made by first brazing two thin stainless-steel tubes in two through holes in a 1.33-in. con-flat flange. We then placed two 2.5-m optical fiber pigtail cables [made by dividing single-mode (P1-3224-FC-5, Thorlabs) and multimode (M15L05, Thorlabs) fiber patch cables], with their jackets and claddings removed, in the holes and sealed the outer openings of the tubes with Torr-Seal. The feedthroughs made in this way showed no leak down to 1×10^{-10} Torr in a helium leak test. The optical fiber connectors of the pigtail cables are secured by mating couplers in a supporting bracket fixed to the flange.

The head-side end of the single-mode fiber for the laser is placed inside a custom-made focus lens assembly. First we passed the core of the fiber through a glass capillary [250 μm inner diameter (i.d.)] taken out of a fiber splice (TS125, Thorlabs) and cleaved the end using a commercial fiber cleaver. If the beam profile is a clean Gaussian, the fiber is glued to the glass capillary with 0.6$\sim$1 mm of the fiber protruding from the end of the capillary. The glass capillary is inserted snugly (by a small Inconel wire spring) to a duralumin fiber holder attached to the laser planar piezomotor. The focus lens is an aspheric lens (NT46-361, Edmund Optics) with an effective focal length of 2 mm and an outer diameter of 3 mm. It is mounted on a fine-threaded lens tube that fits the threads of the fiber holder. By rotating the lens tube against the friction generated by the helical Inconel spring we can fine adjust the distance between the fiber and the lens to be slightly larger than the focal length, and can focus a Gaussian beam on the cantilever with a sufficiently small diameter ($<$15 μm). The quadrant photodiode (SD085-23-21-021, Advanced Photonix) is tested in a helium storage Dewar and mounted on a planar piezomotor using an adjustable fixture that can give translation and tilt for the initial coarse beam spot positioning. When we optimally focus the laser beam on the cantilever, the reflected beam spot on the photodiode becomes circular with a diameter of $\sim$1.2 mm.

To facilitate the positioning of the sample with respect to the tip and the alignment of the laser beam on the cantilever, we designed a high-resolution plan-view CCD optics using the main chamber as the lens tube, as shown schematically in Fig. 4. To achieve the maximum numerical aperture, we mounted an objective lens (NT32-724, Edmund Optics) with

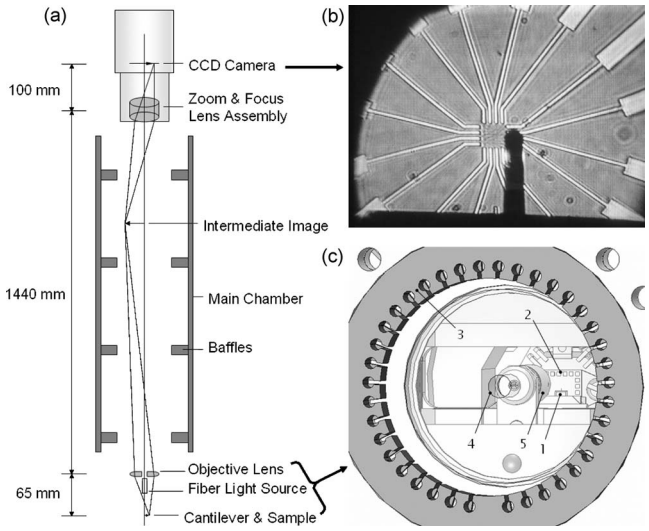

FIG. 4. (a) Schematics of CCD optics. The illuminating light source (the cleaved end of a multimode optical fiber) is located on a side of the lower end of the laser lens assembly. Its light is reflected off the target (the sample and the cantilever) and directed toward the CCD camera achieving bright-field mode operation. (b) A snapshot of the CCD vision showing the patterned sample surface and the cantilever. (c) A slightly tilted top-view of the LTAFM head showing (1) the cantilever and (2) the sample through the objective lens (no lens refraction is assumed in this illustration). (3) Wire guide ring, (4) hole in the objective lens, (5) laser lens assembly.

25 mm diam and 60 mm focal length on top of the head. We drilled a small hole (4 mm diam) in the lens along its optical axis to allow for the unhindered piezomotor-driven motion of the optical fibers. The intermediate image of the tip and the sample formed near the top of the main chamber is refocused onto the CCD by a telescopic microscope lens. The field of view can be controlled from 40 μm$\times$60 μm to 200 μm $\times$300 μm by adjusting the zoom of the telescopic microscope lens. To provide a white light source illuminating the sample area of interest for the CCD vision, we glued a fixture that holds the cleaved end of the multimode fiber on one side of the laser lens fixture. Observation of various patterned samples showed that the CCD optics has a resolution of $\sim$1.5 μm, which is smaller than the *XY* scanner range (2 μm at 5 K) and much larger than the sample *XY* piezomotor step size ($\sim$10 nm at 5 K). It can thus provide sufficient detail to adjust the tip position on the sample area of interest as well as to focus the laser on the cantilever. With the wide range of the field of view and the high resolution of the CCD vision, no special marker patterns are required in order to locate the transport target because the photolithography-generated parts of the electrodes surrounding the transport target can be utilized as markers.

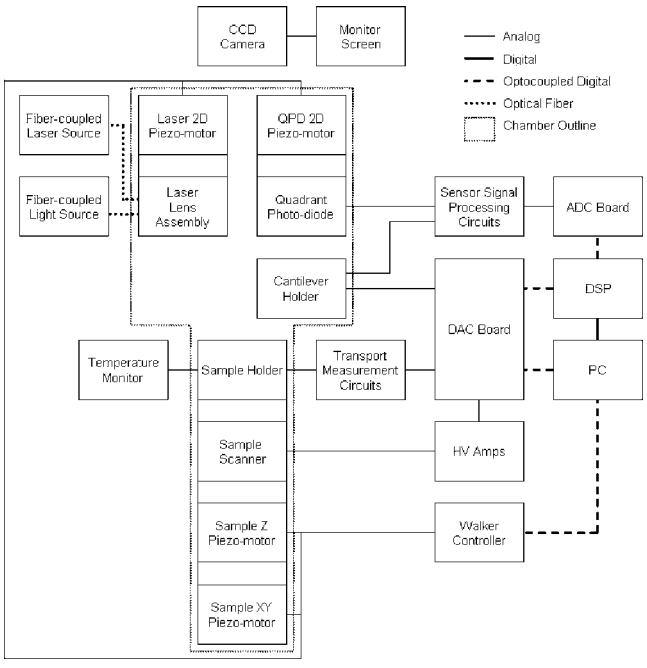

FIG. 5. Block diagram of LTAFM control system.

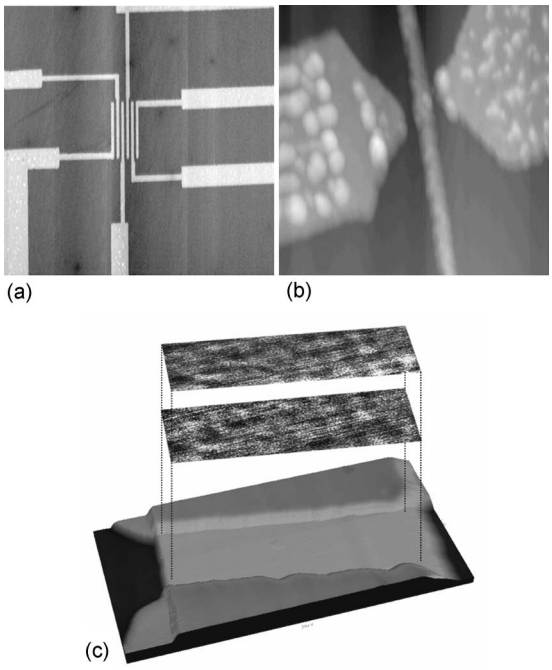

FIG. 6. (a) Amplitude-modulation mode topography of 50-nm-thick gold electrodes patterned on silicon oxide surface (2 μm$\times$2 μm, 5 K). (b) Frequency-modulation mode topography of 20-nm-thick gold electrodes patterned on silicon oxide surface (0.4 μm$\times$0.4 μm, 5 K). (c) Tip-gated conductance maps of a GaAs HEMT device at 5 K with tip bias voltage +2V (top) and −2V (middle), and simultaneously taken contact-mode topography (bottom, 1 μm$\times$2 μm). The grayscale for the conductance map is from 0.65 μS (black) to 0.69 μS (white) at a drain to source bias of 100 mV.

III. EXPERIMENT AND RESULTS

In all of the experiments described below we used a homemade digital signal processor (DSP)-based feedback controller that can perform a 32-bit proportional-integral-derivative (P-I-D) feedback operation at a 60 kHz sampling rate, as shown schematically in Fig. 5. In the electronics design, special care was taken to eliminate ground loops formed by multiple signal cables and to decouple the analog ground from the noisy digital ground. All analog-to-digital converters (ADCs) and digital-to-analog converters (DACs) in the rack-mounted high-voltage (HV)-DAC box and the chamber-mounted preamp box are optically coupled to the digital control signals from the control boards. All analog signal cables were double-shielded with a single thick copper

braid tube that provided a solid grounding between the chamber and the control rack. We programmed the scanning probe microscope (SPM) control and image-processing software in Visual C++ using Microsoft Foundation Class (MFC) framework and OpenGL library.

We tested the capability of the microscope to locate a sample area of interest using two different silicon-oxide/silicon samples with patterned Au/Ti electrodes as shown in Fig. 6. After moving the sample with the 2D piezomotor guided by the CCD vision, only two to three scans (at low and medium zoom levels) were required to find and zoom into the exact location of interest on the sample. With the stabilized laser source and the CCD illumination turned off, the thermal drift was less than 0.2 nm per hour in the X-Y and Z directions.

To test the tip-gated transport measurement capability, we used a GaAs-based high electron mobility transistor (HEMT) device as the 2DEG transport sample and measured the conductance as a function of the position of the voltage-biased tip at 5 K. We were able to observe the bias-dependent spatial inhomogeneity of the conductance map caused by a defect-induced potential disorder affecting the 2DEG flow.

IV. DISCUSSION

We have developed and successfully demonstrated the performance of a versatile and Dewar-immersion type cryogenic atomic force microscope with full *in situ* piezomotor controls, high-resolution plan-view CCD vision, and the tip-gated transport measurement capability. Local transport properties of nanometer-sized objects, such as 0D/1D/semi-2D quantum confinement systems made of semiconductors, metals, and/or organic compounds can be studied with this system utilizing the local tip gating effect achieved by applying a bias voltage to the conducting tip. If combined with a superconducting magnet Dewar, this system can be used as an ideal scanned-gate microscope system for tip-gated transport studies under a magnetic field. With the use of a piezoresistive cantilever or tuning fork, we can use the laser as an independent position-adjustable optical excitation source for the study of optoelectronic transport device with position-controlled laser illumination.

ACKNOWLEDGMENT

This work was supported by the Creative Research Initiatives Program of Korean Ministry of Science and Technology.

[1] G. Binning, C. F. Quate, and Ch. Gerber, Phys. Rev. Lett. **56**, 930 (1986).
[2] S. Manne, H. J. Butt, S. A. C. Gould, and P. K. Hansma, Appl. Phys. Lett. **56**, 1758 (1990).
[3] M. A. Topinka, B. J. LeRoy, S. E. J. Shaw, E. J. Heller, R. M. Westervelt, K. D. Maranowski, and A. C. Gossard, Science **289**, 2323 (2000).
[4] M. T. Woodside and P. L. McEuen, Science **296**, 1098 (2002).
[5] W. Han, S. M. Lindsay, M. Dlakic, and R. E. Harrington, Nature **386**, 563 (1997).
[6] M. Rief, H. Clausen-Schaumann, and H. E. Gaub, Nat. Struct. Biol. **6**, 346 (1999).
[7] S. Fowler, R. Best, J. L. Toca-Herrera, T. Rutherford, A. Steward, E. Paci, M. Karplus, and J. Clarke, J. Mol. Biol. **322**, 841 (2002).
[8] L. Howald, E. Meyer, R. Lüthi, H. Haefke, R. Overney, H. Rudin, and H.-J. Güntherodt, Appl. Phys. Lett. **63**, 117 (1993).
[9] F. J. Giessibl and B. M. Trafas, Rev. Sci. Instrum. **65**, 1923 (1994).
[10] A. Radenovic, E. Bystrenova, L. Libioulle, M. Taborelli, J. A. DeRose, and G. Dietler, Rev. Sci. Instrum. **74**, 1022 (2003).
[11] K. Yokoyama, T. Ochi, T. Uchihashi, M. Ashino, Y. Sugawara, N. Suehira, and S. Morita, Rev. Sci. Instrum. **71**, 128 (2000).
[12] N. Suehira, Y. Tomiyoshi, Y. Sugawara, and S. Morita, Rev. Sci. Instrum. **72**, 2971 (2001).
[13] B. W. Alphenaar, K. Tsukagoshi, and M. Wagner, J. Appl. Phys. **89**, 6863 (2001).
[14] E. D. Minot, Y. Yaish, V. Sazonova, and P. L. McEuen, Nature **428**, 536 (2004).
[15] S. H. Pan, E. W. Hudson, and J. C. Davis, Rev. Sci. Instrum. **70**, 1459 (1999).